3 Results

3.1 PKA compartmentalization in the heart

3.1.1 Localization of AKAP18δ in cardiac tissue

In this study, the expression of AKAPs in heart tissue, especially in SR-enriched fractions, is investigated. By immunoprecipitation with AKAP18 δ isoform specific antibodies, Western blot analysis and cAMP agarose precipitation one of the expressed AKAPs is identified as the δ-isoform of AKAP18. Immunofluorescence studies and electron microscopy of cardiac tissue reveal the localizaltion of AKAP18δ in the SR, and its co-localization with SR proteins.

3.1.1.1 AKAP18δ is expressed in rat heart

In order to investigate the expression of AKAPs in the heart, homogenates of adult and neonatal heart are prepared. After SDS-PAGE and transfer to a PVDF membrane, a RII-overlay assay is performed (Fig. 3.1.1 A). The RII-overlay, as previously described by Carr and Scott (Carr and Scott, 1992), is a modified Western blot method for detection of AKAPs. In both homogenates (adult and neonatal rat heart), signals for AKAPs of different sizes are detected. At 50 kDa, a signal is detected, which corresponds to the apparent molecular weight of AKAP18δ. The signals diminish after treatment with the PKA anchoring disruptor peptide S-L314E, showing that the signals are specific for AKAPs. For further identification of the 50 kDa AKAP, the homogenates are subjected to Western blotting with the antibody A18δ4, specifically recognizing AKAP18δ (Henn et al., 2004) (Fig.3.1.1 B). The antibody recognizes a signal at 50 kDa, showing that AKAP18δ is present in neonatal and adult heart homogenates. The antibody A18δ4 recognizes an additional RII-binding protein of about 55 kDa. The identity of this protein is currently not known.

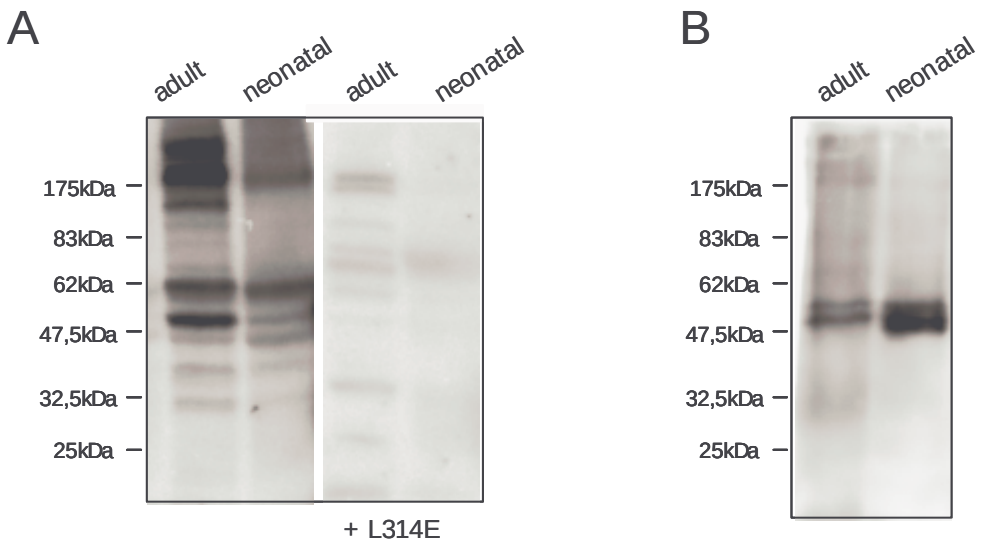

Figure 3.1.1 AKAP18δ is present in rat heart homogenates Homogenates from adult and neonatal rat heart are prepared and detected **A**, by RII-overlay in absence (left panel A) or presence (right panel A) of 10 nM L314E anchoring disruptor peptide, and **B**, detected by Western blotting with the anti-AKAP18δ specific antibody A18δ4.

3.1.1.2 AKAP18δ is immunoprecipitated from rat heart homogenate

Figure 3.1.2 shows an immunoprecipitation (IP) of AKAP18δ from total rat heart homogenate. The IP is performed with different antibodies against AKAP18. Antibody A18δ4 recognizes only splice variant δ of AKAP18, antibody A18δ3 recognizes additionally splice variant γ, and antibody 1964 detects all known AKAP18 splice variants because its epitope in the C-terminus is common to all AKAP18 splice variants (table 2, material and methods). AKAPs in the precipitate are detected by RII-overlay. Detection by Western blot is not possible, because AKAP18δ migrates in the SDS-PAGE at the same size as the heavy chains of the antibody used for the precipitation. All three antibodies immunoprecipitate a prominent 50 kDa RII-binding protein, which corresponds in size to recombinant AKAP18δ. The preimmune serum does not precipitate the proteins. AKAP18δ can be precipitated also from neonatal heart homogenate, and from cultured neonatal cardiac myocytes using antibody A18δ4 (Fig 3.1.2 C and D).

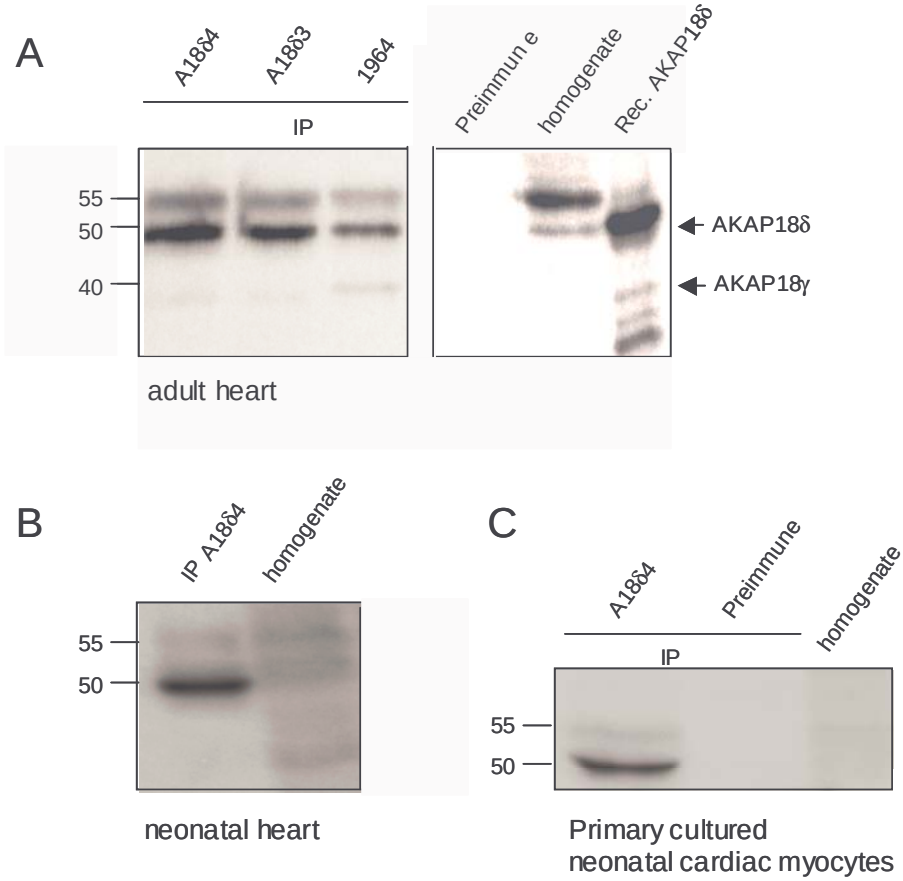

Figure 3.1.2 AKAP18 δ is immunoprecipitated from rat heart Immunoprecipitation (IP) with antibody A18δ4, A18δ3, 1964 or preimmune serum **A** from adult rat heart left ventricle, **B** from neonatal heart homogenate, **C** from primary cultured neonatal cardiac myocytes. The homogenates and precipitates are probed in RII-overlay assays.

3.1.1.3 cAMP agarose precipitation pulls down AKAP18δ from rat heart homogenate

To examine whether AKAP18δ forms a complex with PKA in the heart, cAMP-agarose pull-down experiments with rat left ventricle homogenates are carried out (Fig. 3.1.3). Cyclic AMP-agarose efficiently pulls down RII subunits (Fig. 3.1.3, C) and a protein recognized by antibody A18δ4, (Fig. 3.1.3, B). The precipitated protein corresponds in size approximately to recombinant AKAP18δ, suggesting that it represents the endogenous AKAP18δ. Rec AKAP18δ runs slightly different from the expected size of 50 kDa on SDS-PAGE, because of the presence of a short HA tag. As a control, cAMP-agarose pull-down experiments are carried out in the presence of cAMP. Under this condition, neither RII subunits (Fig. 3.1.3) nor AKAP18δ are detectable in the

precipitate (Fig. 3.1.3, A, lane 2). For further control of the Western blot, fractions (~20%) of the pull-down experiment samples are subjected to RII-overlay and proteins of the similar size as with antibody A18δ4 can be detected (Fig. 3.1.3, A).

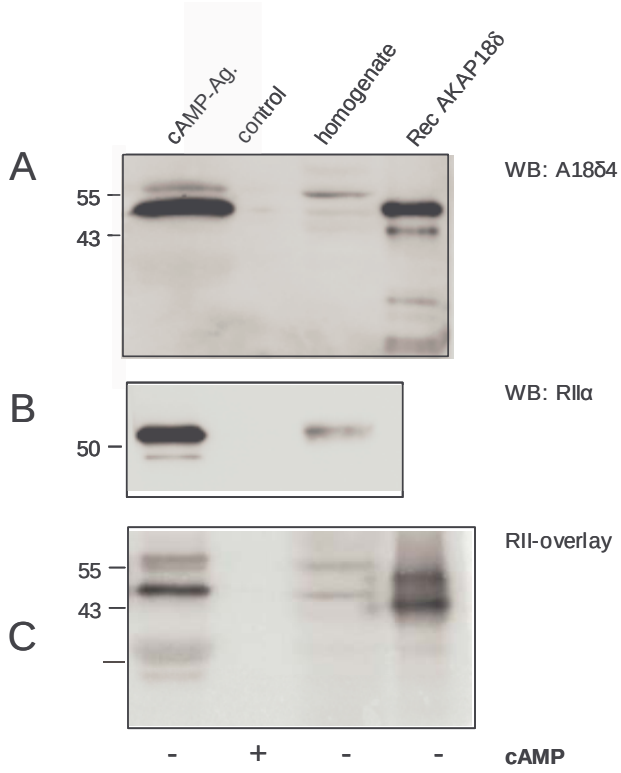

Figure 3.1.3 AKAP18 δ forms a complex with PKA in the heart Cyclic AMP-agarose precipitates are obtained from adult rat heart homogenate in the absence or presence of cAMP. The precipitates are subjected to **A**, RII overlay, and **B**, AKAP18δ is detected with antibody A18δ4. **C**, RIIα subunits are detected by Western blotting.

3.1.1.4 AKAP18δ is found in fractions of enriched SR

To see in which part of the cardiac myocyte AKAP18δ is expressed, adult rat heart homogenate is fractionated by centrifugation through a sucrose gradient and fractions are detected by RII overlay. The enrichment of SR proteins is controlled by Western blotting with antibodies directed against calsequestrin, a marker for the SR. In fraction 10 and 11, the strongest signal for calsequestrin can be detected, showing that they are highly enriched in SR proteins (Fig.3.1.4, A). RII-overlay detection shows that especially fractions 10 and 11, contain RII-binding proteins with mobilities of >200 and ~110, 90, 60 and 50

kDa. These proteins are not detectable if RII subunits are preincubated with 500 nM anchoring disruptor peptide Ht31 (see 2.1.4), indicating that the detected proteins represent AKAPs, (Fig.3.1.4, A). To further determine the identity of the RII-binding proteins, immunoreactivity to different AKAP antibodies are tested. Immunoblotting of the heart fractions with antibody A18δ4 revealed the presence of AKAP18δ in SR enriched fractions as well as in fractions 4-6. If antibody A18δ4 is preincubated with the peptide used for immunization, these signals disappear (Fig.3.1.4, B). PKA regulatory RI, RII and catalytic subunits can be detected in all fractions of heart homogenates (Fig.3.1.4, C) (Lygren et al., 2007).

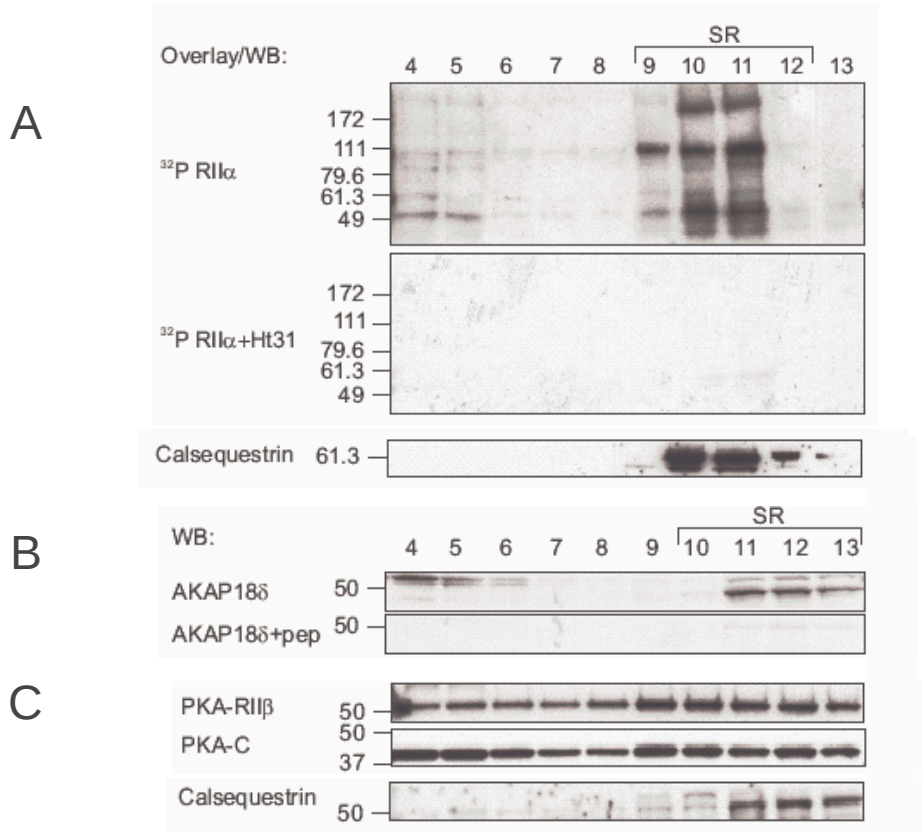

Figure 3.1.4 AKAP18δ is present in heart sarcoplasmatic reticulum A, Rat heart SR fractions are subjected to RII overlay as a probe in absence (upper panel) or presence (middle panel) of 500 nM Ht31 anchoring disruptor peptide. **B**, The same fractions are analyzed by immunoblot for calsequestrin (a major Ca^{2+} binding protein of SR) (lower panels). Detection of AKAP18δ in rat heart SR fractions by Western blotting. Pep: A18δ4 antibody is preincubated with the peptide used for immunization. **C**, Detection of regulatory (RIα, RIIα and RIIβ) and catalytic (C) subunits of PKA in SR fractions.

3.1.1.5 Immunolocalization of AKAP18δ to the SR in adult rat heart

AKAP18δ is detected using indirect immunofluorescence and laser scanning microscopy in cryostat sections of rapidly frozen left ventricle from adult rat hearts. In longitudinal sections, staining with the AKAP18δ-specific A18δ4 antibody (Fig. 3.1.5) shows in addition to a diffuse distribution in the cytosol, a strong signal localized in thin parallel striations. Co-staining with a monoclonal antibody to the z-line specific protein α-actinin (Geiger et al., 1981), shows in the overlay image (yellow signal), that the AKAP18δ distribution corresponds to that of α-actinin. Detection with the A18δ3 antibody, recognizing AKAP18δ and γ isoforms, yields a localization in striated pattern twice as narrow as using the AKAP18δ-specific A18δ4 antibody (Fig. 3.1.5, a, left panel, red signal). Every second striation overlaps with α-actinin staining. RII subunits localize also in longitudinal sections of the heart tissue. RIIα staining (Fig. 3.1.5, c middle panel) shows a similar pattern as the AKAP18δ staining. In the superimposed image of RIIα/AKAP18δ staining, the majority of the AKAP18δ and RIIα staining overlaps (Fig. 3.1.5, c right panel). Most important, SERCA2a and PLB co-localizes with AKAP18δ. SERCA2a, PLB and AKAP18δ staining is found in a periodic (about 2µm) transverse pattern. The results suggest that AKAP18δ is localized close to SERCA2a and PLB at the z-lines, which contain the junctional SR .

Staining of neonatal cardiac myocytes with the AKAP18δ-specific A18δ4 antibody (Fig. 3.1.6 red signal) (Lygren et al., 2007) shows as in adult cardiac tissue, a strong signal localized in thin parallel striations. Co-staining with α-actinin reveals that AKAP18δ distribution corresponds to that of α-actinin. Thus, also in neonatal myocytes, AKAP18δ is localized to the sarcomeric z-lines.

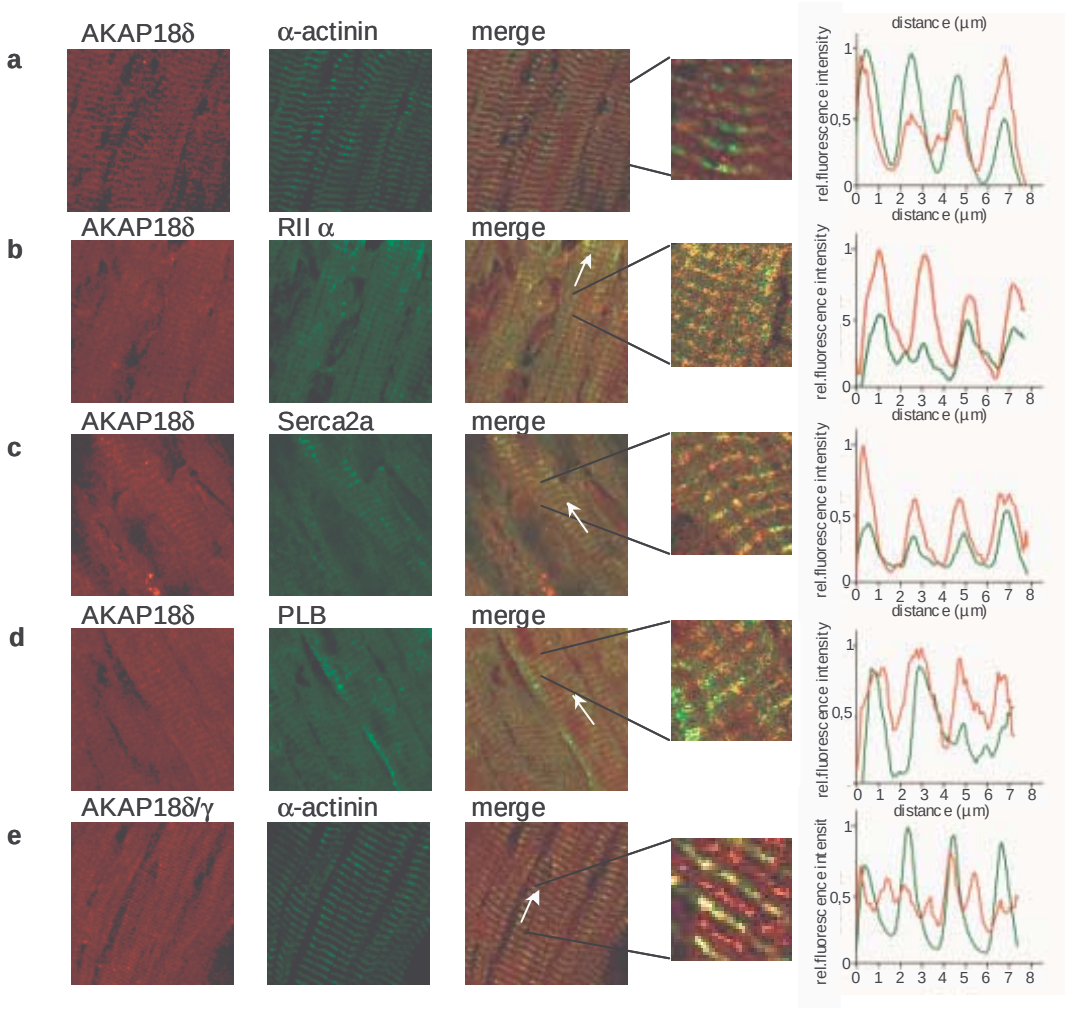

Figure 3.1.5 AKAP18δ and PKA co-localize with SERCA2a and PLB in heart tissue. Rat heart tissue sections are immunostained for AKAP18δ and AKAP18γ,δ (red, Cy3-labeled secondary antibody) in combination with α-actinin, PKA-RIIα, 2 and PLB (green, Cy5-labeled secondary antibody). The relative fluorescence intensities along an axis perpendicular to the orientation of sarcomeres are measured (right panel). Scale bar 20 µm.

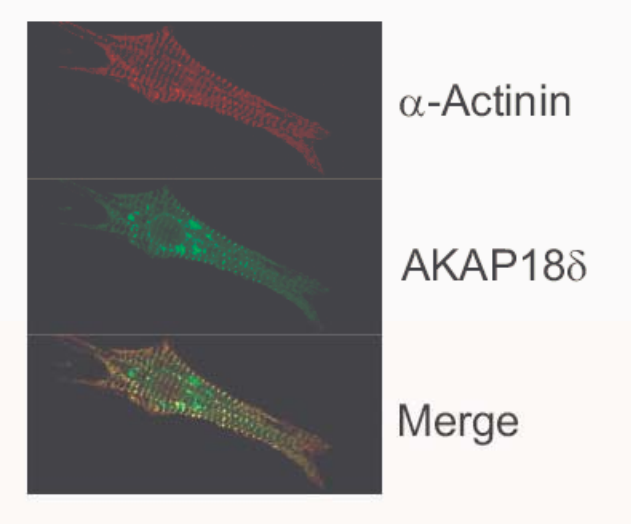

Figure 3.1.6 AKAP18δ co-localize with α-actinin in neonatal cardiac myocytes. Primary cultured neonatal cardiac myocytes immunostained for AKAP18δ (red, Cy3-labeled secondary antibody) in combination with α-actinin (green, Cy5-labeled secondary antibody).

3.1.1.6 AKAP18δ, PLB and SERCA2a are detected in close proximity by immunoelectron microscopy (EM)

The co-localization of PLB, SERCA2a and AKAP18δ is confirmed by electron microscopy (EM) with sections from neonatal cardiac myocytes after immunogold staining using specific antibodies labeled with two different sizes of gold particles (Fig. 3.1.7). Labeled AKAP18δ, SERCA2a and PLB are detectable in the same cellular compartment. The striations seen in the images are the myofibrils. Labeled AKAP18δ, SERCA2a and PLB, are found on stacks of SR that are interspersed with the contractile machinery. In Fig. 3.1.6 A, co-localization of SERCA2a and PLB particles is shown. Immunogold-labeled AKAP18δ is detected in close proximity of SERCA2a (Fig.3.1.7 B), or PLB (Fig.3.1.7 C), on the same SR membranes. Evaluation of 50 images reveals that more than 20 % of PLB and SERCA2a, more than 10 % of AKAP18δ and SERCA2a and more than 12 % of the PLB and AKAP18δ co-localizes within distances of less than 60 nm. This analysis supports the co-localization observed by immunofluorescence microscopy and suggests that a complex of AKAP18δ, SERCA2a and PLB is formed (Lygren et al., 2007).

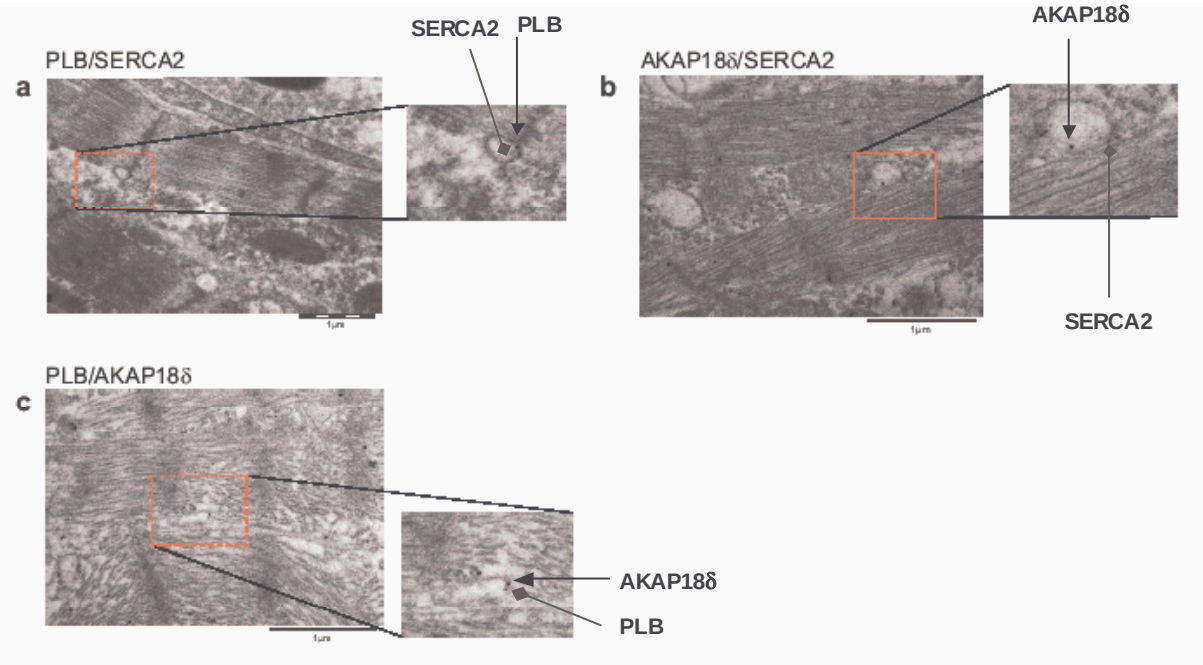

Figure 3.1.7 AKAP18δ, SERCA2a and PLB co-localize on the SR in neonatal cardiac myocytes. Immunogold staining of **A,** PLB (15 nm) and SERCA2a (10 nm), **B**, co-staining of SERCA2a (12 nm) and AKAP18δ (18 nm), and **C**, co-staining of PLB (10 nm) and AKAP18δ (15 nm) is shown. Secondary antibodies labeled with gold particles of different sizes are used to allow detection of double staining. Scale bars, 1 µm. The magnified views show representative areas where the indicated proteins co-localize.

The previously described experiments prove, that AKAP18δ is expressed at the SR of adult and neonatal rat cardiac myocytes.

3.1.2 Interaction between AKAP18δ and PLB

Co-precipitation studies with rat heart homogenates and with lysates of transfected HEK293 cells co-expressing PLB and AKAP18δ show, that PLB and AKAP18δ form a complex. Peptide spot technology in combination with RII-overlay assay and transfection of different PLB-constructs are performed to map the binding site.

3.1.2.1 PLB and AKAP18δ co-immunoprecipitate

Adult left ventricle and neonatal rat hearts are homogenized, and an immunoprecipitation of AKAP18δ with the A18δ4 antibody (Fig.3.1.8, A) is performed (Lygren et al., 2007). Western blotting with an antibody specific against PLB shows a signal of around 6,5 kDa (the size of the PLB monomer) in the immunoprecipitates with antibody A18δ4, in the immunoprecipitates with the PLB antibody 2D12 and in the homogenate. Boiling of the samples with DTT before SDS-PAGE dissociates the PLB pentamer, so only monomeric PLB at around 6,5 kDa is detected. Immunoprecipitation with rat preimmune serum and α-actinin do not yield any signal for PLB in the Western blot. The RII-overlay assay confirms that antibody A18δ4 precipitates AKAP18δ, but no signal for AKAP18δ is detected in the precipitate with the PLB antibody (Fig. 3.1.8, B). Co-immunoprecipitation of endogenous AKAP18δ and PLB using PLB antibody is not possible, because the epitope for the PLB antibody overlaps the AKAP18δ interaction site and presumably competitively inhibits the interaction. This experiment shows, that AKAP18δ and PLB can be co-immunoprecipitated and detected from neonatal rat heart homogenate.

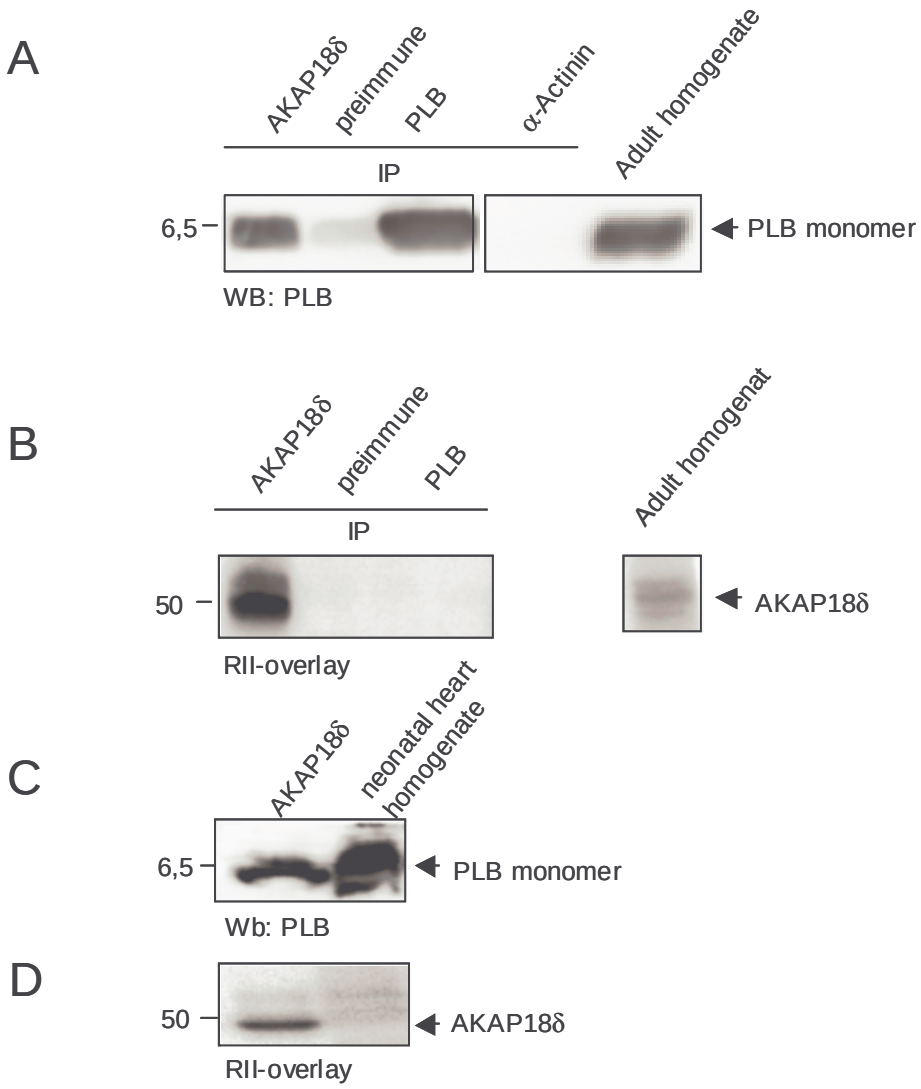

Figure 3.1.8 AKAP18δ associates with PLB in heart homogenates Adult rat heart homogenates are subjected to immunoprecipitation with antibody A18δ4, rabbit preimmune serum, PLB and α-actinin antibodies. Homogenates and immunoprecipitates are analyzed by **A**, Western blot for the presence of PLB monomers, and **B,** by RII-overlay to confirm the immunoprecipitation of AKAP18δ. Neonatal rat heart homogenates are subjected to immunoprecipitation with antibody A18δ4, and analyzed by **C**, Western blot using PLB antibody, and **D,** by RII-overlay for detection of AKAP18δ.

Immunoprecipitation experiments show, that in cardiac myocytes, PLB and AKAP18δ are forming a complex, or by direct interaction, or by a common intermediate protein.

3.1.2.2 AKAP18δ and PLB interact directly

To investigate whether PLB and AKAP18δ interact directly and to map the interaction sites, SPOT technique and overlay assay are carried out. Amino acid residues 1-36 of PLB are synthesized as 20-mer peptides with 2 amino acid-offset on cellulose membranes. Membranes are analyzed for AKAP18δ binding by overlay with purified, recombinant GST-AKAP18δ protein, followed by anti-GST immunoblotting. GST alone is used as a negative control.

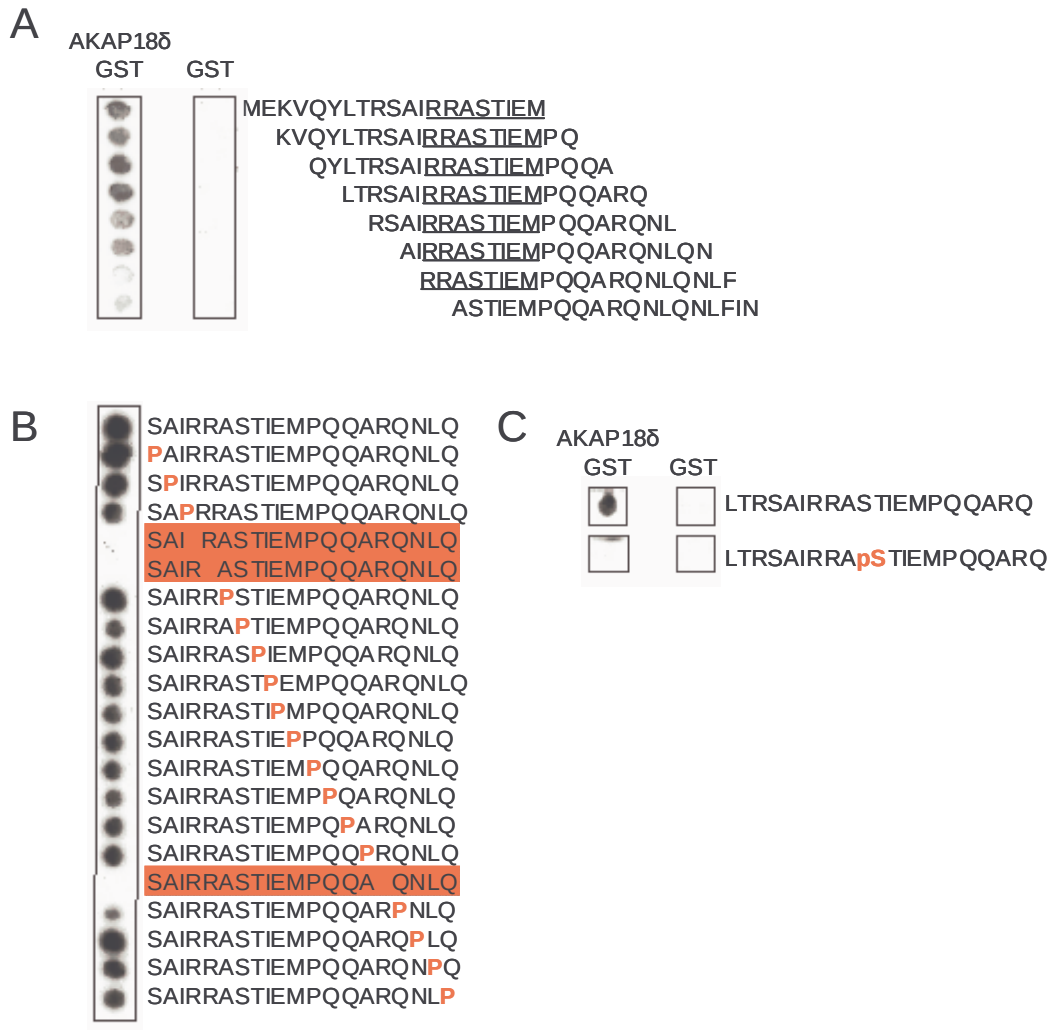

Figure 3.1.9 AKAP18δ binds PLB directly. A SPOT synthesis of PLB amino residues 1-36 and detection by overlay with AKAP18δ-GST and following Western blotting against GST. PLB synthetic peptides are spotted with 2 amino acids offset. GST protein is used as negative control. Underlined amino acids indicate amino residues relevant for AKAP18δ-PLB binding. **B**, AKAP18δ binding to PLB mutated with proline (P) in each position from 10 to 29 is analyzed by GST-AKAP18δ overlay. **C**, PLB peptides with or without phosphorylated S16 (pS) are subjected to AKAP18δ-GST overlay experiments.

Spots showing a signal in the overlay assay contain important amino acids for the PLB-AKAP18δ interaction (Fig. 3.1.9, A). These synthesized peptides contain the common amino acid sequence RRASTIEM. Substitution of the amino acids I13 and R14 as well as substitution of R25 to prolin, (destroying the α-helical structure of the cytosolic part of PLB), disrupts the binding of AKAP18δ to the PLB sequence (Fig 3.1.9, B). Mimicking PKA phosphorylation by synthesis of phosphorylated S16 (pS) also disrupts AKAP18δ binding to the peptide (Fig. 3.1.9, C) (Lygren et al., 2007).

3.1.2.3 Overexpressed PLB and AKAP18δ co-immunoprecipitate in co-transfected HEK293 cells

In order to further confirm with an independent approach the region of the AKAP18δ/PLB interaction site, we generate clones of YFP-tagged wild type and truncated AKAP18δ in the pEYFP-N1 vector, and clones of PLB in the pEYFP-C1 vector. Additionally, AKAP18δ is cloned in a fusion vector between pEYFP-N1 and pEYFP-C1 allowing expression of untagged protein, (see material and methods, chapter 2.2).

To see if the co-expressed full-length proteins in HEK293 cells show the same co-immunoprecipitation as endogenous PLB and AKAP18δ, HEK293 cells are transiently transfected with PLB-YFP and AKAP18δ-YFP fusion constructs, and cell lysates are prepared after 24 h for immunoprecipitation as described before. Detection by Western blotting against PLB shows a clear signal for PLB around 40 kDa in the immunoprecipitates of AKAP18δ (Fig. 3.1.10, A). In the precipitate with the PLB antibody 2D12 as well as in the lysate of transfected cells, a signal of 40 kDa is detected by immunoblotting for PLB (fusion protein PLB monomer and YFP). Using preimmune serum instead of the antibody for immunoprecipitation does not yield a signal in the Western blot. To verify the expression of AKAP18δ-YFP in the cells as well as to see the efficiency of the AKAP18δ precipitation, we detect the same samples with the antibody A18δ4 recognizing AKAP18δ. A signal of around 80 kDa (fusion protein AKAP18δ and YFP) is detected in the immunoprecipitation of AKAP18δ and in the lysate.

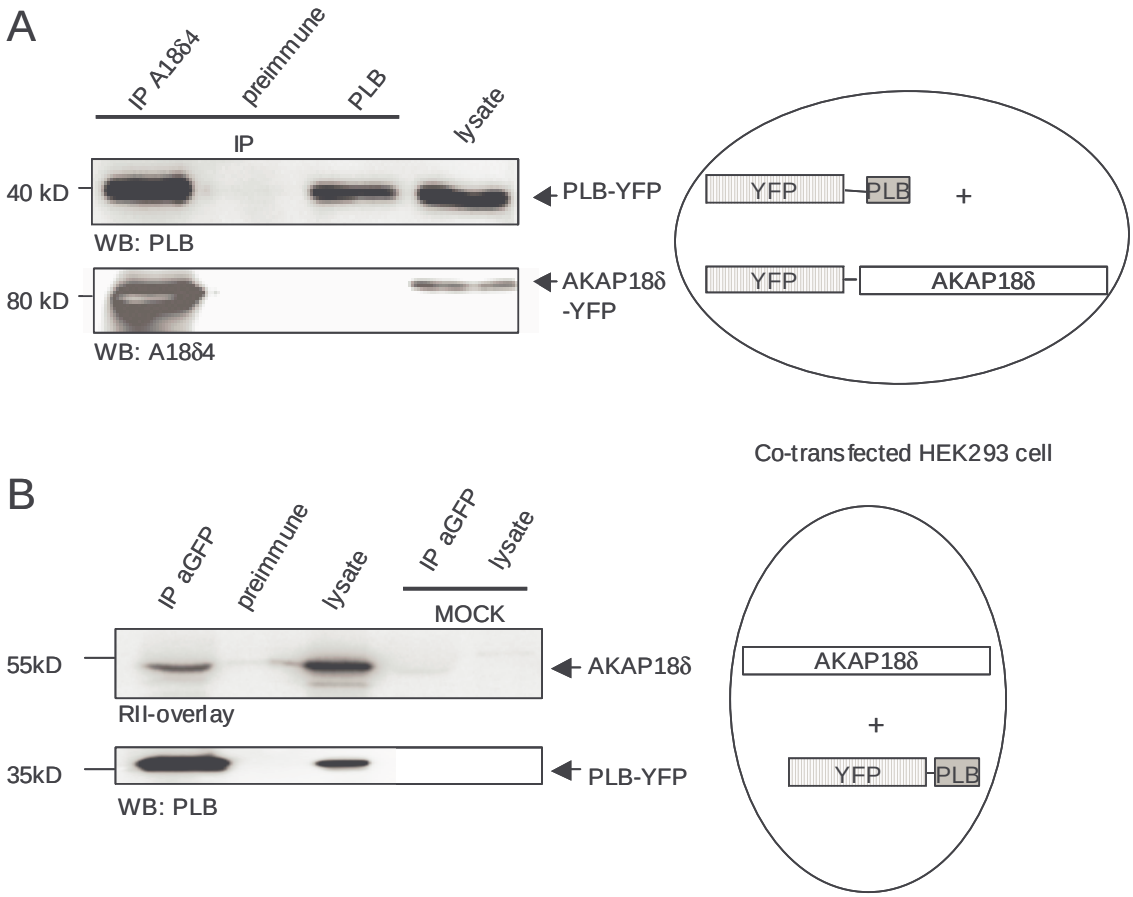

Figure 3.1.10 AKAP18δ interacts with PLB. **A**, HEK293 cells are transfected with expression vectors encoding AKAP18δ and PLB fused to YFP. Lysates are subjected to immunoprecipitation with A18δ4 antibody and precipitates and lysates are analyzed by immunoblotting for the presence of YFP-AKAP18δ and YFP-PLB. **B**, HEK293 cells are transfected with expression vectors encoding untagged AKAP18δ and PLB fused to YFP. Lysates are subjected to immunoprecipitation with anti-GFP-GST antibody and precipitates and lysates are analyzed by immunoblotting for the presence of YFP-PLB and by RII-overlay for detection of AKAP18δ. Untransfected cells are used as negative control.

In rat heart homogenate co-immunoprecipitation of endogenous AKAP18δ and PLB using PLB antibody is not possible because binding of the PLB antibody stearical hinders AKAP18δ binding (Fig.3.1.8 B). Using tagged proteins, precipitation of PLB by targeting the YFP tag allows the whole PLB protein for interaction with AKAP18δ. Co-transfection of YFP-tagged PLB and untagged AKAP18δ vector constructs in HEK293 cells and following immunoprecipitation with rabbit polyclonal aGFP-GST antibody 02 (recognizing also YFP and CFP) are performed. After precipitation of PLB-YFP, a protein of around 50 kDa, the

size of AKAP18δ, is detected by RII-overlay (Fig. 3.1.10, B). This 50 kDa signal appears in the lysate, but is not detectable with preimmune serum or immunoprecipitate from lysate of untransfected (MOCK) cells. This indicates, that untagged AKAP18δ is co-precipitated with the PLB-YFP fusion protein. To verify the expression of PLB-YFP and to see the efficiency of the PLB-YFP precipitation, we detect the same samples with the PLB antibody. A signal of around 40 kDa (fusion protein of the PLB monomer of around 6,5 kDa and YFP of around 27 kDa) is detected in the IP of PLB-YFP and in the lysate.

3.1.2.4 PLB-YFP deletion and substitution construct binding to AKAP18δ

To investigate further the AKAP18δ binding site of PLB, several substitution and deletion mutants of YFP fused PLB are co-transfected together with untagged AKAP18δ in HEK293 cells (Fig. 3.1.11, A). The recombinant proteins are immunoprecipitated with the GFP02 antibody and detected by RII-overlay. The RII-overlay shows AKAP18δ binding to the N-terminal PLB deletion mutants (Fig. 3.1.11, B). Contradictory to our expectations, the construct PLB-N26-YFP, containing only the membrane part of PLB co-precipitates AKAP18δ, whether the C-terminal C30-PLB-YFP construct, containing only the cytosolic part of PLB, does not co-precipitate AKAP18δ. Substitution of amino acids L13, R14 and R25 to prolin (P), does not affect the co-precipitation of AKAP18δ with PLB, in difference to the results obtained in the peptide spotting experiment. Introducing mutations in the membrane part on L31 and L37, responsible for SERCA2a regulation and pentamer formation, abolishes co-precipitation of AKAP18δ, proposing that the membrane part of PLB is important for AKAP18δ binding. Western blotting for YFP shows that similar amounts of PLB-YFP constructs are immunoprecipitated (Fig. 3.1.11, B).

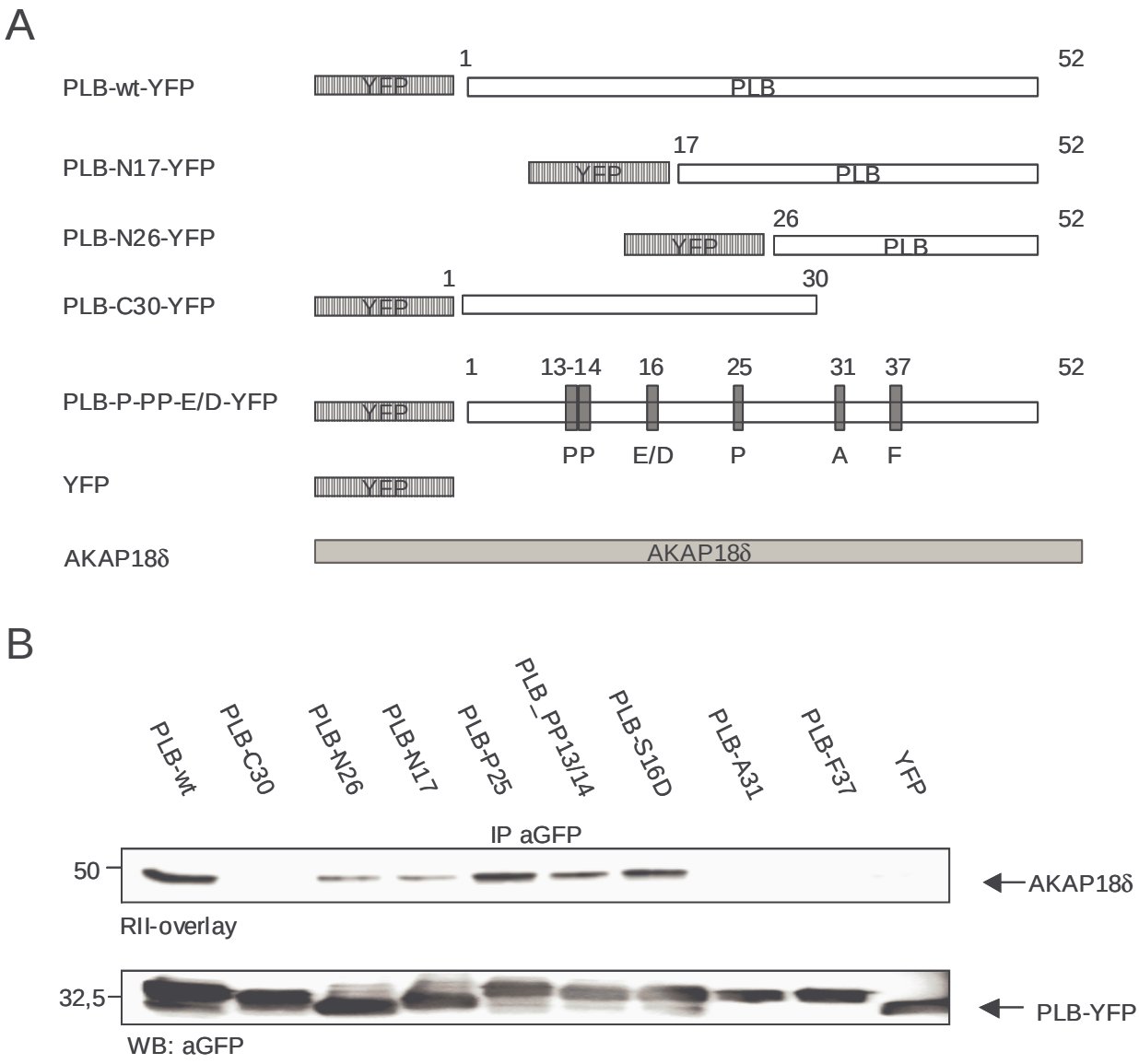

Figure 3.1.11 Co-IP of AKAP18δ and PLB-YFP. **A**, Scheme of PLB deletion and substitution constructs. Numbers indicate amino acid residues of PLB. **B**, HEK293 cells are transfected with expression vectors encoding untagged AKAP18δ and the indicated PLB-constructs fused to YFP. Lysates are subjected to immunoprecipitation with anti-GFP antibody. Precipitates are analyzed by immunoblot for the presence of YFP-PLB and for detection of AKAP18δ by RII-overlay.

3.1.2.5 N-terminal AKAP18δ-YFP deletion constructs bind PLB-YFP

To investigate and map the binding site for PLB in AKAP18δ, studies with AKAP18δ deletion constructs are carried out in HEK293 cells (Fig.3.1.12). The amino terminus of AKAP18δ is truncated stepwise, and the constructs are co-expressed with PLB-YFP in HEK293 cells (Fig.3.1.12, A).

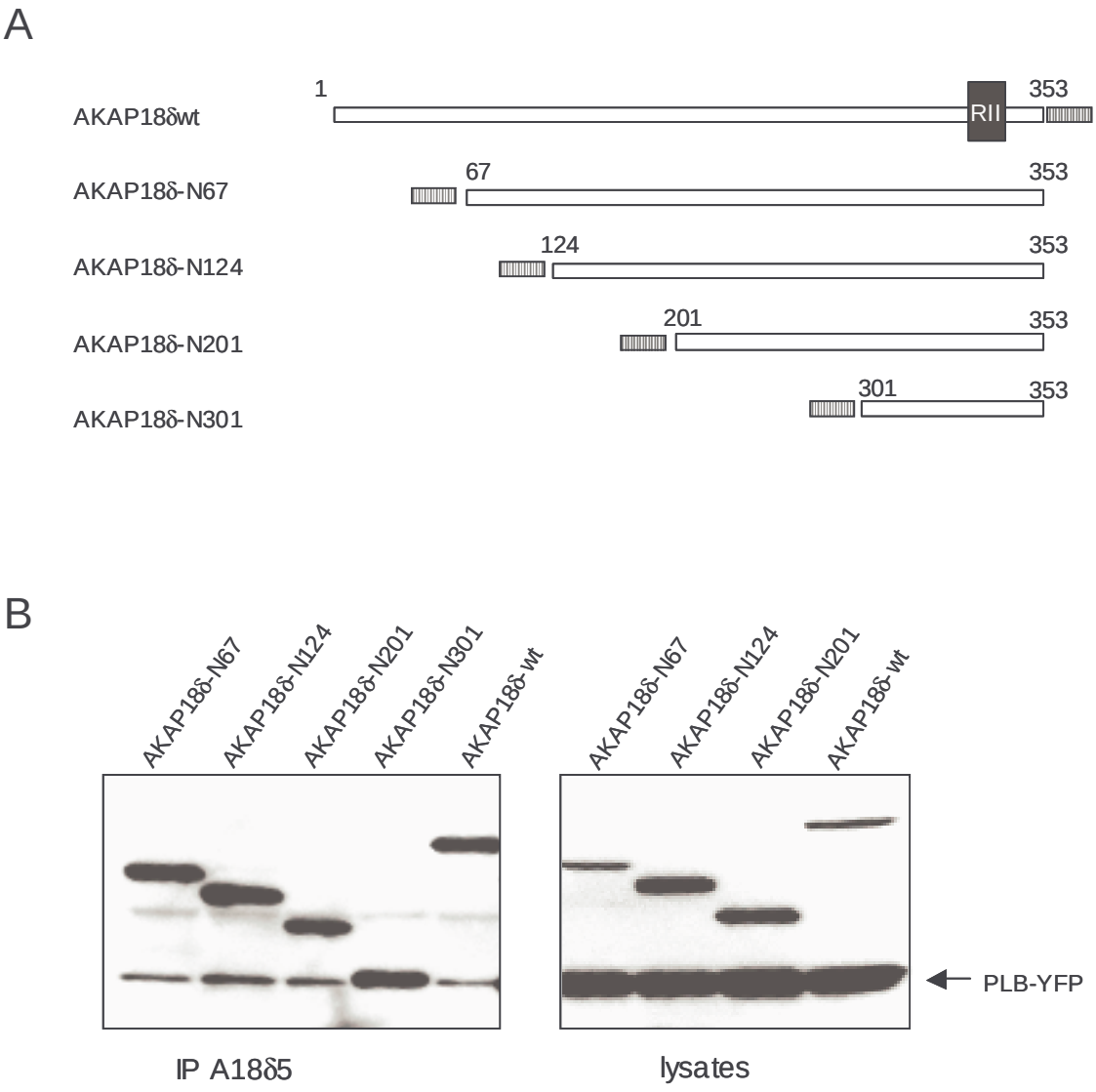

Figure 3.1.12 Co-IP of AKAP18δ deletion constructs and PLB-YFP. A HEK293 cells are transfected with expression vectors encoding AKAP18δ deletion constructs and PLB fused to YFP. **B** Lysates are subjected to immunoprecipitation with the A18δ5 antibody recognizing all AKAP18 constructs. Precipitates are analyzed by Western blot with antibody aGFP for the presence of YFP-PLB and AKAP18δ-YFP.

After precipitating with antibody A18δ5, we detect co-precipitation of PLB-YFP and AKAP18-YFP deletion constructs for full length AKAP18δ, AKAP18δ-N67, AKAP18δ-N124, AKAP18δ-N201 and AKAP18δ-N301 by Western blotting for the YFP tag. Antibody A18δ5 is directed against the whole AKAP18δ protein and therefore able to recognize all AKAP18δ deletion constructs and AKAP18 isoforms. Detection of the cell lysates shows, that in all samples, PLB-YFP and AKAP18 deletion constructs are expressed (Fig.3.1.12, B). This indicates, that the N-terminal amino residues are not essential for the PLB/AKAP18δ binding.

3.1.2.6 Influence of PLB phosphorylation on the binding

In the peptide SPOT experiment phosphorylation of PLB S16 abolishes AKAP18δ binding. To verify the influence of PLB phosphorylation on the AKAP18δ binding in vivo, adult rat hearts are homogenized, and an immunoprecipitation of AKAP18δ with the A18δ4 antibody is performed. Lysis buffer for heart homogenates is used with and without phosphatase inhibitors. Phosphatase inhibitors stop dephosphorylation by phosphatases and allow detection of S16 PLB. Samples are analysed for total and S16 phosphorylated PLB by Western blotting with antibodies recognizing all PLB or only S16 phosphorylated PLB. After addition of phosphatase inhibitors, phospho-PLB co-precipitates with AKAP18δ, whereas without inhibitors, PLB can hardly be detected (Fig. 3.1.13, A). In the lysate and after precipitation with the PLB antibody 2D12 as positive control, phospho-PLB is detected in samples supplemented with phosphatase inhibitors and surprisingly also in the absence of phosphatase inhibitors. Total PLB is detected in all samples except after precipitating with preimmune serum as negative control (Fig. 3.1.13, B). AKAP18δ is precipitated with A18δ4 antibody in similar amounts with and without phosphatase inhibitors, (Fig. 3.1.13, C). Contradictory to the peptide spotting experiment, where phosphorylation of S16 abolishes binding to AKAP18δ, in heart homogenate also phosphorylated PLB is co-precipitated with AKAP18δ.

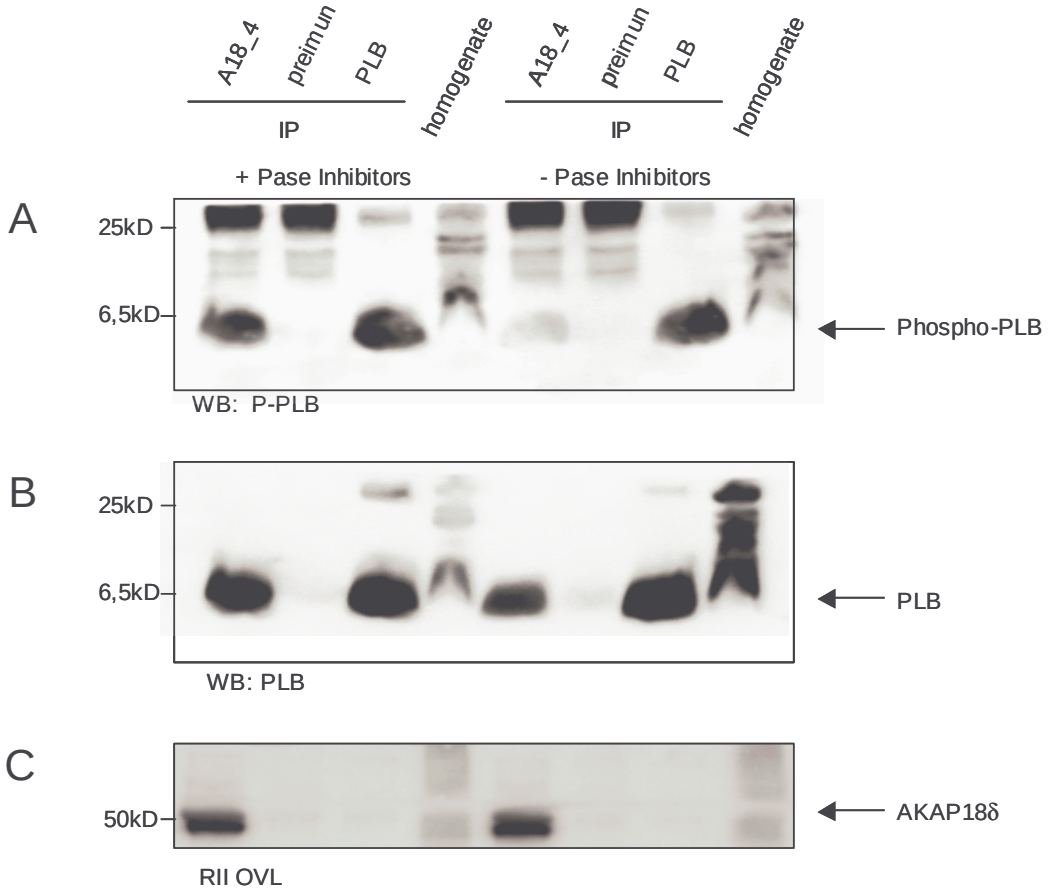

Figure 3.1.13 AKAP18δ associates with phospho-PLB in heart homogenates Adult rat heart homogenates are subjected to immunoprecipitation with antibody A18δ4, control rabbit preimmune serum and PLB antibody in the presence and absence of phosphatase inhibitors. Homogenates and immunoprecipitates are analyzed by immunoblotting for the presence of A, phospho-PLB, B, total PLB, and C, by RII-overlay to control the immunoprecipitation of AKAP18δ.

3.1.3 Influence of AKAP18δ on the Ca^{2+}re-uptake in the heart

To investigate the function of AKAP18δ tethering PKA to the PLB-SERCA2a complex in the cardiac myocyte, the laboratory of Manuela Zaccolo at the Telethon institute in Padua examines the consequence of reduced AKAP18δ expression on the Ca^{2+} re-uptake into the cardiac SR. AKAP18δ is knocked down in neonatal cardiac myocytes using siRNA, (Fig. 3.1.14, C; siRNA efficacy tested in HaCaT cells) and Ca^{2+} re-uptake is measured. Cy3-labeled siRNA is injected into neonatal cardiac myocytes together with a plasmid encoding the FRET-based Ca^{2+}-sensor D1ER, which is located to the SR. The SR is Ca^{2+}-depleted by blocking SERCA2a with 2,5-Di-*tert*-butylhydroquinone (BHQ), a reversible inhibitor, in Ca^{2+}-free solution. BHQ is washed out, Ca^{2+} is added, and Ca^{2+} re-uptake is detected by the FRET-based Ca^{2+}-sensor in Cy3-positive cells in the absence or presence of the ß-AR agonist norepinephrine (NE) (Fig. 3.1.14, A). Fig 3.1.14 C shows the averages of time constants τ, calculated by fitting the fluorescence changes during the Ca^{2+} re-uptake phase, represented in A. Comparing AKAP18δ siRNA transfected (green lines) to non transfected (red lines) or control siRNA transfected cells (blue lines), the Ca^{2+} re-uptake in AKAP18δ siRNA transfected cells, is significantly reduced with and without NE treatment. Comparing stimulated and non-stimulated cells, stimulation with NE increases the Ca^{2+} re-uptake into the SR for control, and control siRNA transfected cells. In AKAP18δ siRNA transfected cells, NE does not increase Ca^{2+} re-uptake to the SR, but even reduces it (Lygren et al., 2007).

AKAP18δ is important for the Ca^{2+} re-uptake into the SR by bringing PKA to PLB and facilitating thereby PLB phosphorylation and its releasing of SERCA2a inhibition, activating the transport of Ca^{2+} into the SR.

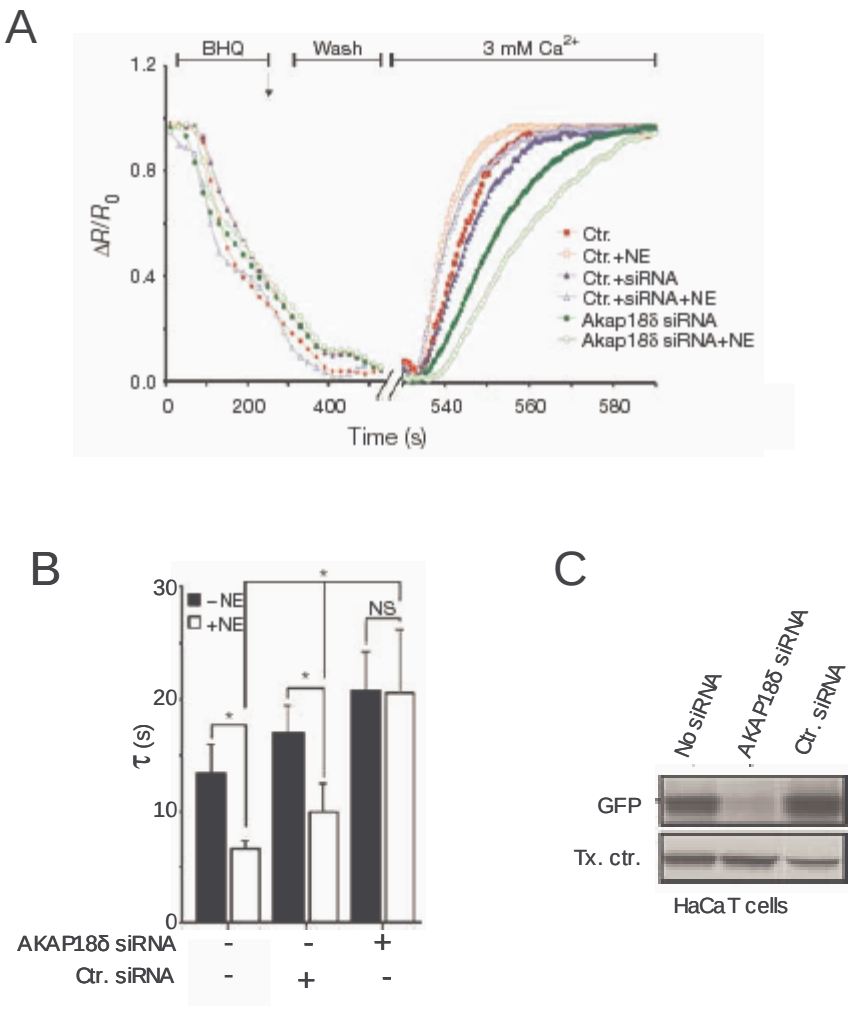

Figure 3.1.14 Disruption of the AKAP18δ-PLB complex influences Ca^{2+} re-uptake in the SR. A Kinetics of Ca^{2+} release and re-uptake subsequent to depletion of Ca^{2+} with 50 mM BHQ in the SR of cardiac myocytes transfected with the D1ER sensor alone (red curves), together with control siRNA (blue curves) or AKAP18δ siRNA (green curves) in the presence (open symbols) or absence (filled symbols) of 10 mM NE (arrow indicates time of NE addition). For clarity only every second data point is shown. Note: time scale differs at break point. **B** The time constant τ (tau) averages are calculated by fitting the recovery phase in the curve of Ca^{2+} re-uptake using the exponential function $f(t) = \sum ni=1\ Ai\ e-t/\tau i + C$ (right). For each sample n > 20 independent cells are examined (*: p < 0.01, Student's t-test; NS: non significant). **C** Western blot: siRNA efficacy tested in easily transfectable HaCaT cells expressing GFP–Akap18d. Tx. ctr.: transfection control, an unrelated Flag-tagged construct (β-arrestin) was co-transfected and detected by anti-Flag to control for transfection and loading.

3.2 Interaction of AKAP18δ and PDE4D3 in co-transfected HEK293 cells

Stefan et al. showed that PDE4D is located on AKAP18δ bearing vesicles in renal collecting duct principal cells (Stefan et al., 2007). Peptide array analyses indicate that AKAP18δ interacts with two surface-exposed sites on the conserved PDE4D catalytic unit (Bolger et al., 2006; Zhang et al., 2004), and 4 potential binding regions for PDE4D3 are detected in AKAP18δ (Stefan et al., 2007).

To confirm peptide spot data for the PDE4D3 binding site in AKAP18δ, studies with AKAP18δ deletion constructs are carried out in HEK293 cells. From previous peptide spotting of PDE4D and overlay with AKAP18δ-GST, four regions of AKAP18δ appear to be involved in the binding: region 1 is between amino acid 51 and 80, region 2 between amino acid 98 and 135, region 3 between amino acid 196-230 and region 4 between residues 291 and 315. In order to test the relevance of the potential interaction sites for the binding, parts of the amino terminus of AKAP18δ are deleted, and mutations are introduced in the potential binding region 1 and 2. These constructs are co-expressed together with full length PDE4D3 fused to vsv tag in HEK293 cells. After precipitating with antibody GFP02, co-precipitation of PDE4D3 and all AKAP18δ deletion constructs apart from AKAP18δ-N301 or YFP alone is detected. Also AKAP18δ-R66E and AKAP18δ-R116A/R120A co-precipitate PDE4D3-vsv. It seems that full length AKAP18δ co-precipitates PDE4D less efficient than the deletion mutants AKAP18δ-N67, AKAP18δ-N124, and AKAP18δ-N201 (Stefan et al., 2007).

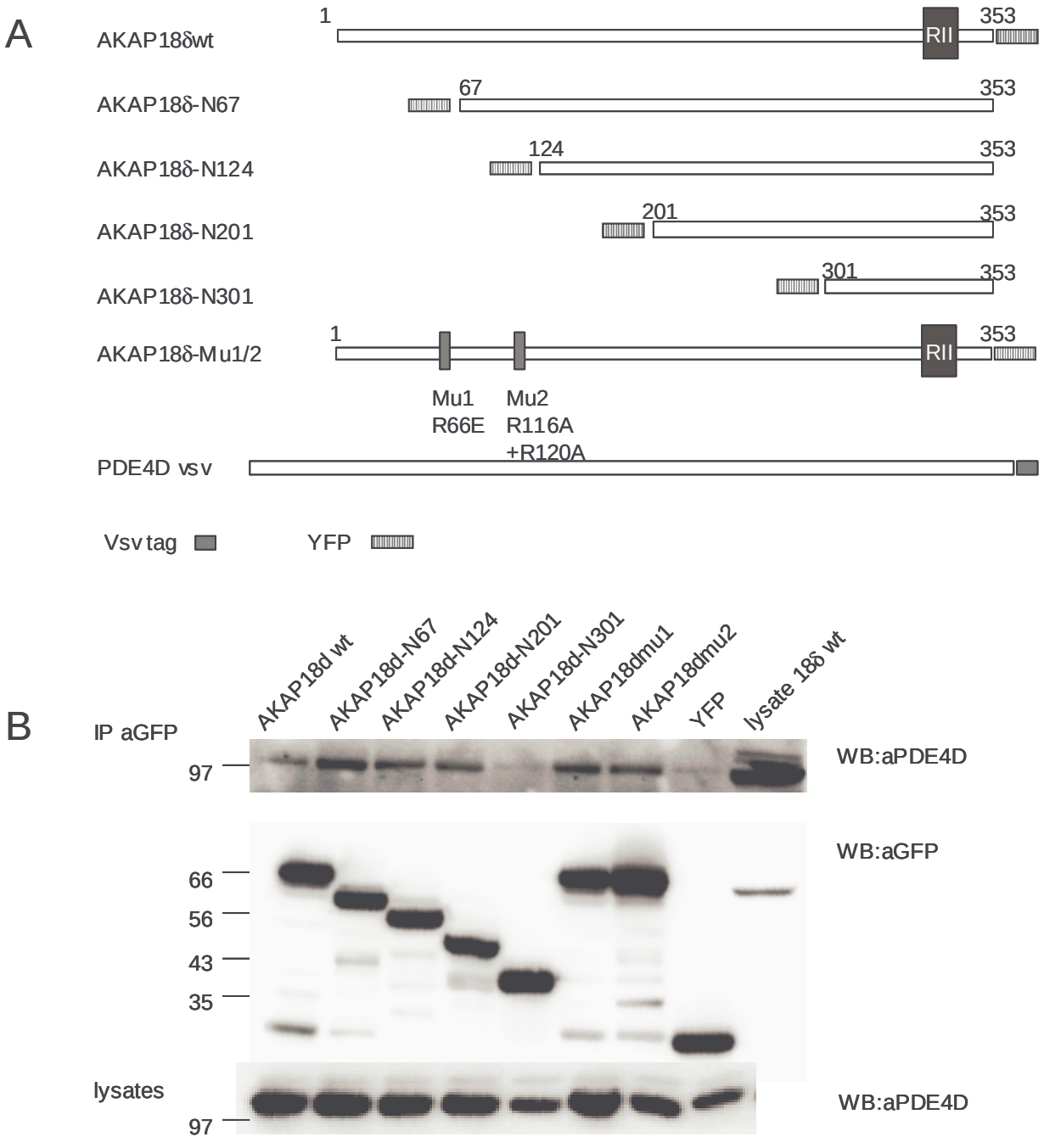

Figure 3.2 HEK293 cells co-expressing PDE4D3-VSV, AKAP18δ-YFP constructs or YFP alone, **A** are subjected to immunoprecipitation (IP) using anti-GFP antibody. The precipitates are analyzed by Western blotting (WB) using anti-GFP and anti-PDE4D antibodies. The expression of PDE4D-VSV is confirmed in lysates by Western blotting.

3.3 Protein kinase A type II activation is sufficient to control the cellular localization of the water channel aquaporin-2 in the kidney

In order to determine whether PKA type I and/or II play/s a role in the AQP2 translocation to the plasma membrane, primary inner medullary collecting duct (IMCD) cells are used. They contain the molecular machinery for the AQP2 translocation. In response to elevation of cAMP through V2R activation by AVP, through activation of adenylyl cyclase with forskolin, or by treatment with dbcAMP, a cAMP analogue non selectively activating PKA types I and II, AQP2 redistributes from intracellular sites to the plasma membrane (Henn et al., 2004; Klussmann et al., 2000; Klussmann and Rosenthal, 2001; Tamma et al., 2001). By selective activation of PKA type II involvment of PKA-R typeI and/or typeII is investigated (manuscript in preparation).

3.3.1 Selective activation of PKA type II is sufficient to elicit the AQP2 shuttle in renal principal cells

Fig. 3.3.1 A shows the intracellular distribution of AQP2 in control IMCD cells. After treatment with AVP, dbcAMP or a combination of the cAMP analogues Sp-5,6-DCI-cBIMPS and 6-MBC-cAMP, preferentially activating PKA type II, AQP2 is predominantly localized at the plasma membrane. Addition of RP-8-Br-cAMPS, a cAMP analogue preferentially inhibiting PKA type I, does not affect the AQP2 shuttle induced by the treatment with Sp-5,6-DCI-cBIMPS and 6-MBC-cAMP. Quantitative analysis of the immunofluorescence images reveal that either non selective PKA type I and type II activation or selective activation of type II, induces the AQP2 shuttle to the same extent (Fig. 3.3.1 B). The percentage of cells responding to the latter two treatments is similar and non-significantly different from the percentage of cells responding to AVP or dbcAMP with a redistribution of AQP2 (Fig. 3.3.1 C).

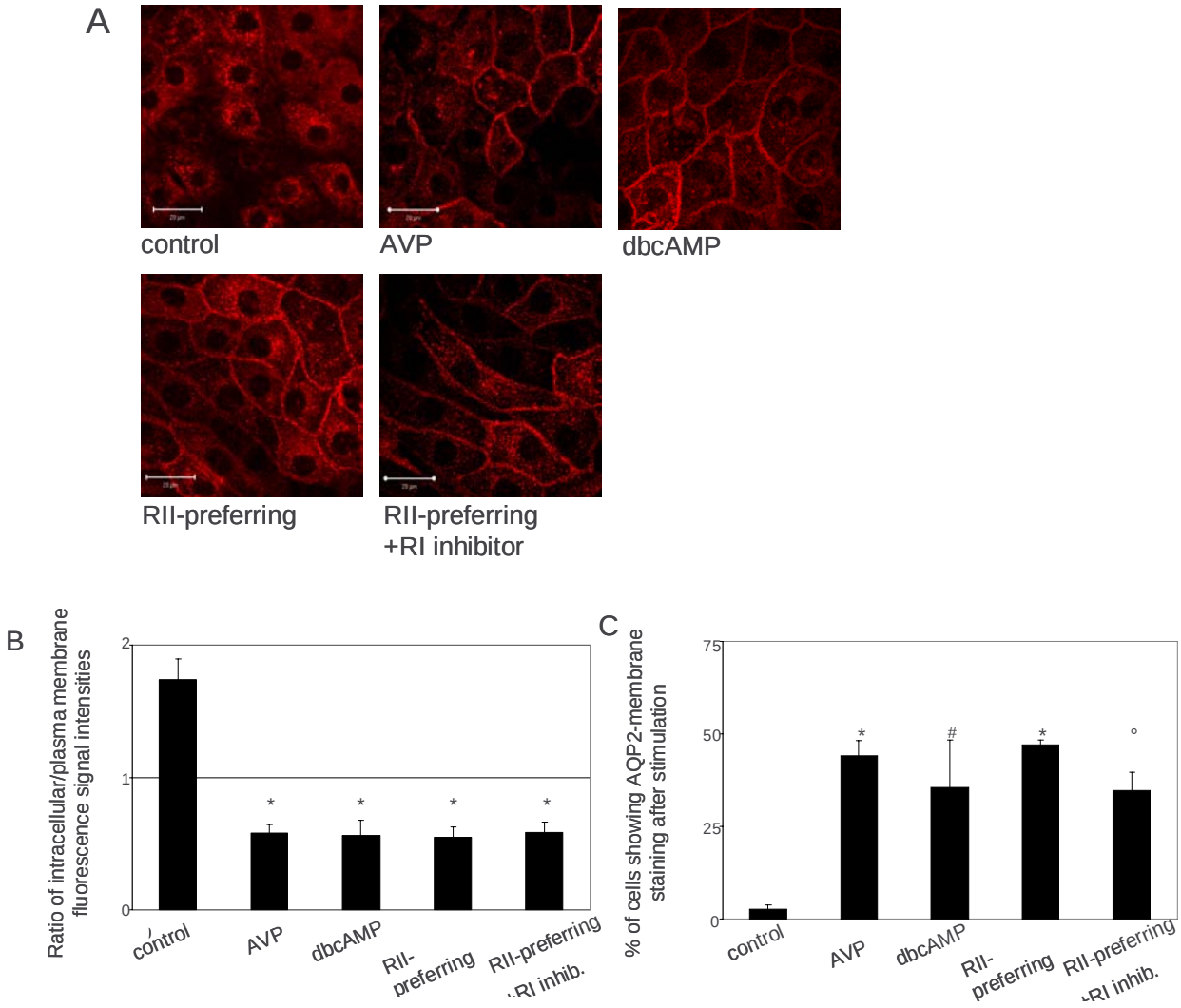

Figure 3.3.1 Selective activation of PKA type II is sufficient to induce the redistribution of AQP2 from intracellular sites to the plasma membrane of IMCD cells. A, Immunofluorescence microscopy of IMCD cells treated with different cAMP analogues. Scale bars, 20 µm. **B**, Quantification of the AQP2 immunofluorescence signals depicted in A. Ratios of intracellular/plasma membrane fluorescence signal intensities are determined (n ≥ 20 cells for each condition; mean ± SD; three independent experiments). A ratio > 1 shows a mainly intracellular localization of AQP2, a ratio < 1 shows a predominant localization at the plasma membrane. *, significantly different from control cells, p < 0,001 (Student's t test). **C**, Percentage of cells responding to the treatments indicated in A with a redistribution of AQP2 to the plasma membrane. The percentage of cells with AQP2 staining at the plasma membrane is obtained by analysis of immunofluorescence microscopic images (> 100 cells per image) from three independent experiments (means ± SD).

3.3.2 AQP2, PKA types I and II reside on the same intracellular vesicles

In IMCD cells, RI and RIIα subunits are detectable by immunoblotting using RI- and RIIα-specific antibodies in the soluble and the particulate (150,000 x *g* pellet) fractions indicating that PKA type I and II are present in both cellular fractions (Fig. 3.3.2 A). Within the particulate fraction, a portion of RII subunits is tethered to AQP2-bearing vesicles by AKAPs (Henn et al., 2004; Hundsrucker et al., 2006; Nedvetsky et al., 2006; Stefan et al., 2007). The presence of RI subunits in the particulate fraction raises the question whether they are also located on AQP2-bearing vesicles.

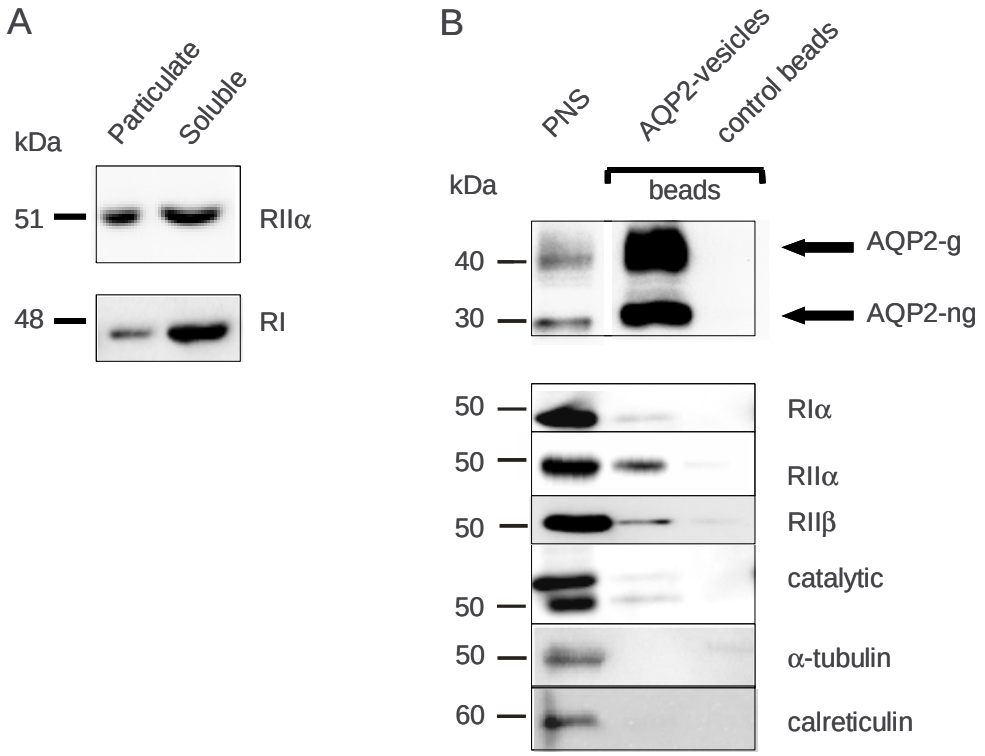

Figure 3.3.2 Both PKA types, I and II, are located on AQP2-bearing vesicles. A, Western blotting of RI and RIIα regulatory PKA subunits in soluble and particulate fractions of IMCD cells. **B**, AQP2-bearing vesicles are prepared from postnuclear supernatants (PNS) of IMCD cells by incubation with AQP2AB beads. As a control, PNS is incubated with control beads. Glycosylated (g) and non glycosylated (ng) AQP2 and tubulin, regulatory RIα, RIIα and RIIβ, and catalytic subunits of PKA are detected by Western blotting.

To this end intracellular vesicles from rat renal inner medullary tissue are immunoisolated with AQP2AB beads. Compared to control beads, regulatory RIIα, RIIβ, RIα and catalytic subunits of PKA, i.e. PKA types I and II, are enriched in the vesicular fraction (Fig. 3.3.2 B). The vesicular fraction does not contain detectable amounts of proteins from other cellular compartments. For example, tubulin, a cytoskeletal protein, or calreticulin, a marker for the endoplasmic reticulum are hardly detectable in the fraction obtained with AQP2AB (Fig. 3.3.2, B). Other markers including COPI (biosynthetic compartment: ER-Golgi transport), GM130 (Golgi) and COXIV (Golgi) are also not detectable (Nedvetsky et al., 2006; Henn et al., 2004; Stefan et al., 2007).

3.3.3 Immunofluorescence microscopy

Immunofluorescence microscopy reveals that in resting IMCD cells RI is distributed throughout the cytoplasm and, in the majority of the cells, also at the plasma membrane. RIIα subunits are found mainly perinuclearly on vesicular or fibre-like structures. The distribution of RI and RII subunits partially overlaps with that of AQP2. After treatment of the cells by dbcAMP, AQP2 staining is mostly detectable in the membrane, as described before (AQP2 translocation). The intracellular distribution of RI and RIIα subunits is not affected by dbcAMP treatment (Fig. 3.3.3).

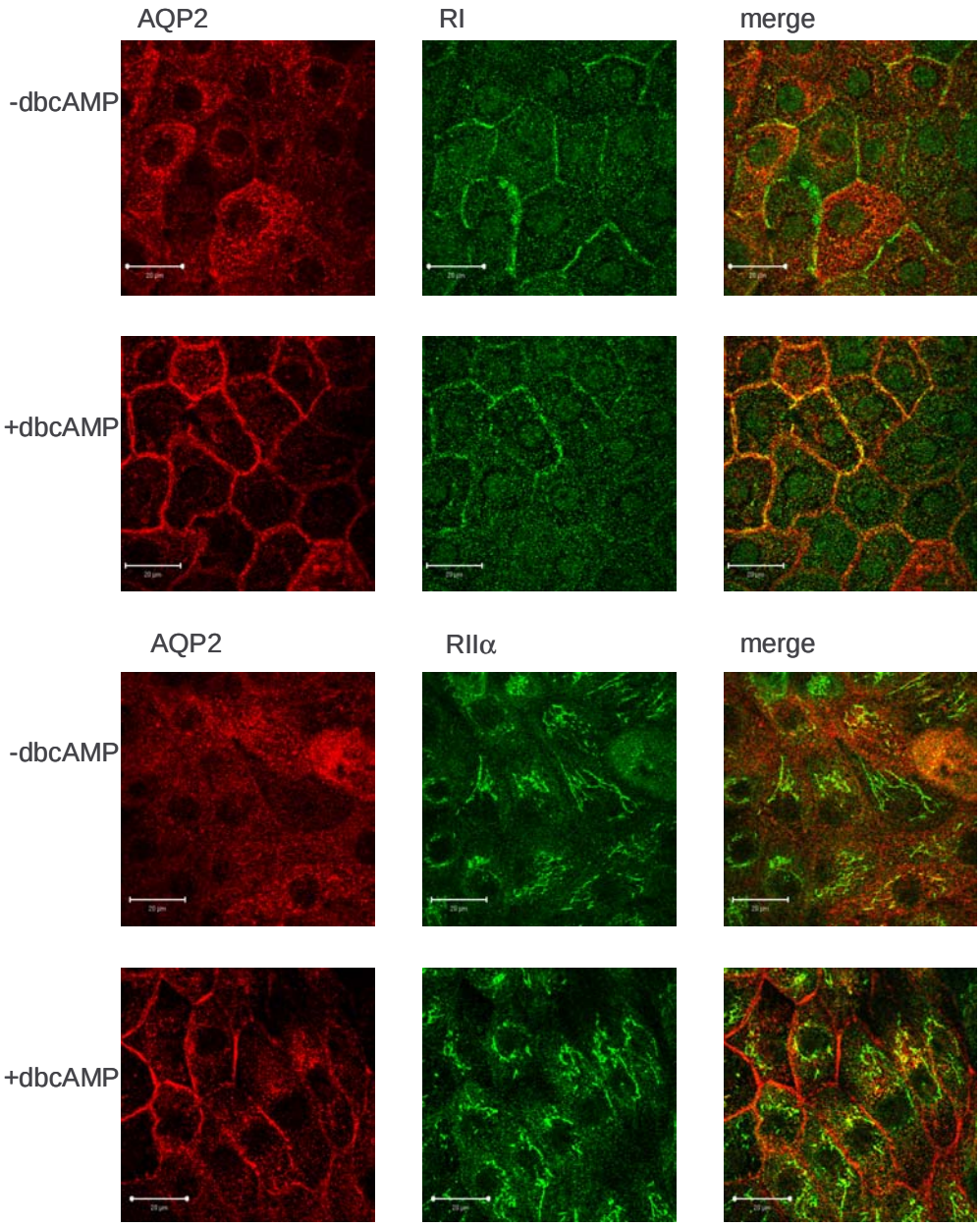

Figure 3.3.3 The localisation of RI and RII regulatory subunits of PKA and AQP2 in resting and dbcAMP-treated IMCD cells. IMCD cells are left untreated or incubated with dbcAMP (100µM, 15 min), fixed and permeabilized. AQP2 and RI and RII subunits of PKA are detected by immunofluorescence microscopy. Scale bars, 20 µm.